



Drought monitoring using the long-term CHIRPS precipitation over Southeastern Iran

Ameneh Mianabadi¹ · Khosro Salari² · Yavar Pourmohamad³

Received: 2 January 2022 / Accepted: 29 May 2022 / Published online: 18 June 2022
© The Author(s) 2022

Abstract

Climate change and global warming are often considered the main reason for water scarcity in Iran. However, there is little evidence showing that the arid/wet regions get drier/wetter due to climate change. Some researchers believe that parts of water challenges in Iran arise from bad governance and mismanagement of water resources. To address the role of climate change on the water scarcity, this study aims to detect the drought trends in the southeast of Iran to investigate drought characteristics changes during 1981–2020. The nonparametric Mann–Kendall test was used for this purpose. CHIRPS product was collected as an alternative source of ground data for trend analysis of drought characteristics. The evaluation metrics show that the CHIRPS product performs better at monthly and annual scales (correlation higher than 0.8) than daily (correlation less than 0.4). The results also illustrate that the duration and severity of short-term droughts (3, 6, and 9 months) have decreased, while their intensity has increased. Conversely, duration, severity, and intensity changes for long-term droughts (12, 18, and 24 months) are insignificant. The trend in the Standardized Precipitation Index (SPI) showed that, in general, the southeast of Iran has not been getting drier during the last four decades. One may conclude that the change in precipitation is not the only reason for water challenges in this area, and both natural and anthropogenic drought might cause water scarcity. Accordingly, it is suggested that the effects of human activities and governmental plans should be considered as well.

Keywords Drought · CHIRPS · Mann–Kendall · Water Scarcity · Human Activities

Introduction

Water scarcity and drying the water bodies in Iran during recent years are often considered as the consequences of climate change/variability and global warming. The report of the World Meteorological Organization, for the period

2001–2010 indicates that Iran has warmed by about 1 °C (WMO 2013) and it will become even drier and hotter in the future (Madani et al. 2016). Some previous studies indicated that global warming would decrease precipitation rates in arid and semiarid regions and increase droughts' intensity, duration, and severity (Heathcote 1983; Xu et al. 2005; UNFCCC 2007; Mahajan and Dodamani 2015; Sharma and Goyal 2020; Pandey et al. 2021). However, Greve et al. (2014) implied there is little evidence to show that the arid regions become drier and wet areas become wetter due to climate change. Some previous studies believed that beside climate change/variability, anthropogenic interventions should be considered as important drivers for water crisis (Ghandehari et al. 2020; Afzal and Ragab 2020; Balist et al. 2022).

It is worth noting that human and nature are coupled (Mianabadi et al. 2015). Considering the climate change/variability as the only reason for the environmental challenges and ignoring the role of human activities allow the policymakers to avoid their own responsibility for dealing

✉ Ameneh Mianabadi
a.mianabadi@kgut.ac.ir; ammianabadi@gmail.com

Khosro Salari
khosrosalari93@gmail.com

Yavar Pourmohamad
yavarpourmohamad@u.boisestate.edu

¹ Department of Ecology, Institute of Science and High Technology and Environmental Sciences, Graduate University of Advanced Technology, Kerman, Iran

² Graduate Student, Water Sciences and Engineering Department, Faculty of Agriculture, Ferdowsi University of Mashhad, Mashhad, Iran

³ Department of Civil Engineering, Boise State University, Boise, ID, USA

with the causes and consequences of the ecological degradation (Oliver-Smith 2012; Safaee et al. 2020).

In Iran, during recent decades, overexploitation of natural resources and the implementation of various development plans such as dam construction and inter-basin water transfer projects have led to environmental degradation in the country (Makhdoum 2008; Kolahi et al. 2012; Eslami et al. 2020). These activities resulted in drying water bodies and declining groundwater resources which in turn led to undesirable consequences such as land subsidence, water contamination, and agricultural losses (Madani 2014; Pourmohamad et al. 2020).

Two of the most important lakes in Iran are located in the southeastern part: Jazmourian wetland on the border of Kerman–Sistan and Balouchestan Provinces and Lake Hamoun on the border of Iran–Afghanistan (See Fig. 1). In recent years, the amount of water in these two lakes has decreased, and sometimes they have been thoroughly dried up (Mianabadi et al. 2022). Drying the lakes has many undesirable economic, social, and environmental consequences, especially in the rural communities (Pourmohamad et al. 2012). From an environmental point of view, drying the lakes causes severe dust storms, which blow toward the surrounding villages and cities (Rashki 2012; Alizadeh-Choobari et al. 2014). It also limits the agricultural activities, resulting in economic problems, unemployment, and migration from rural areas to the cities (Delju et al. 2013; Pourmohamad et al. 2019). Abandoning the rural areas leads to rural population decrease and security threats in both sending and receiving regions (Mianabadi et al. 2021). While these consequences mainly arise from bad governance and a lack of preparedness plans, the government continuously blames climate variability (besides international sanctions) as the leading cause of the current situation (Madani

2014). Accordingly, it is essential to investigate the changes in climate variables in these getting dry areas to assess the role of climate change on the water challenges and drought characteristics.

Previous studies assessed drought trends and their characteristics in some areas worldwide (Pathak and Dodamani 2020; Derdous et al. 2021; Kassaye et al. 2021; Liu et al. 2021; Lotfirad et al. 2021; Qaisrani et al. 2021; Zerouali et al. 2021). Trend analysis of climatic data series requires long-term chronicled data (at least 30 years) (Burroughs 2003). However, the climatic data may not be available sufficiently on both temporal and spatial scales, or the access to the data is restricted. To deal with these limitations, some of the studies investigated the use of satellite precipitation products for trend analysis of drought characteristics (Brasil Neto et al. 2021; Santos et al. 2021). Their results showed that the satellites products performed well for drought monitoring.

Drought trend analysis using the satellite precipitation products did not conduct in any regions in Iran. Thus in this study, we applied the CHIRPS precipitation product (Funk et al. 2015) for drought monitoring as previously used by Guo et al. (2017), Pandey et al. (2021), Najjuma et al. (2021), Sandeep et al. (2021), and Ahmad et al. (2021) with reasonable performance. The CHIRPS product provides long-term precipitation estimates (40 years) and is easily accessible. Some previous studies indicated that the product performed properly in their study regions (Ayehu et al. 2018; Dinku et al. 2018; Gao et al. 2018; Rivera et al. 2018). Hence, it can be a reliable product for drought assessment in the study area. Accordingly, this paper aims to detect the trends in drought in southeastern Iran by using the CHIRPS product to see how the drought characteristics are changing in this area over the last four decades.

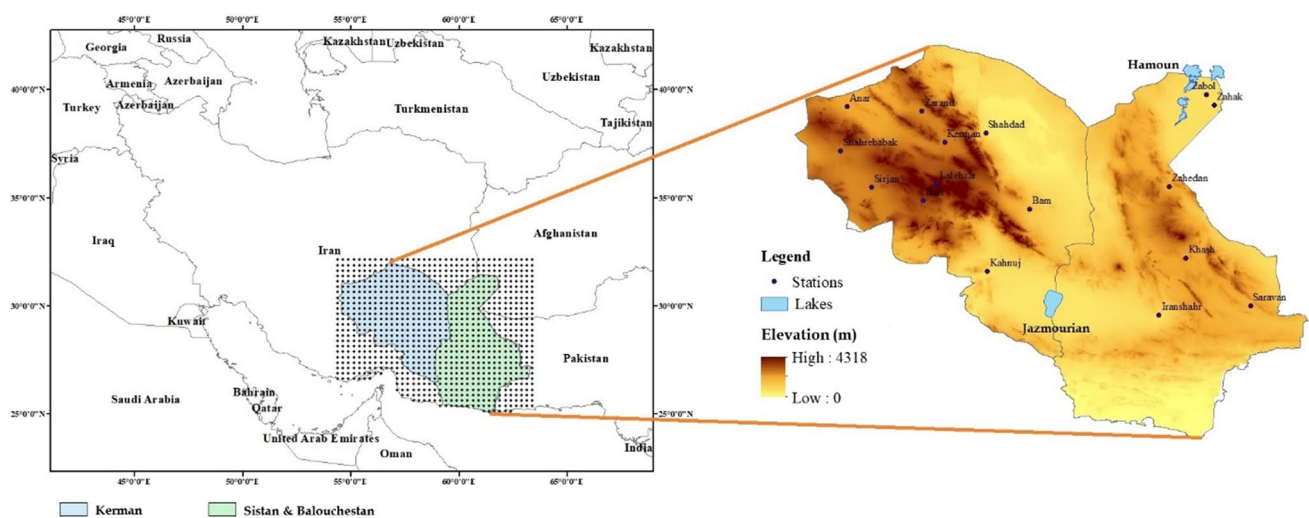


Fig. 1 The study area with the spatial distribution of the CHIRPS grids and the rain gauges

Materials and methods

Study area

The southeast of Iran includes two provinces: Kerman and Sistan and Balouchestan (Fig. 1). These two provinces cover an area of about 365,000 Km² and are classified as arid and semiarid regions. The Lut desert, the hottest spot in Iran (and in the world, according to NASA’s satellite data of land surface temperature (Zhao et al. 2021)), is located in this area. The mean annual precipitation recorded in the capitals of the provinces, Kerman and Zahedan, during 1966–2015 has been about 136 and 80 mm, respectively (Mianabadi et al. 2019). Precipitation occurs mainly in winter, February, and rarely in summer, September (Fig. S1). The mean annual temperature at these two stations is about 15.9 °C and 18.7 °C, with annual potential evaporation of 2560 and 2281 mm, respectively (Mianabadi et al. 2019). In this region, the elevation ranges from zero on the beach of the Oman Sea to more than 4000 m in the mountainous areas in Kerman (Fig. 1).

Synoptic data

Due to limited access to the rainfall data and excluding the time series with missing data, the daily precipitation was only available from 2005 to 2019 for 16 synoptic stations (Fig. 1). The available data were applied to evaluate the accuracy of the CHIRPS product in estimating daily, monthly, and annual precipitation over the study area.

CHIRPS

The Climate Hazards Group InfraRed Precipitation with Station data (CHIRPS; Funk et al. (2015)) was developed based on global Cold Cloud Duration (CCD) rainfall estimates calibrated by the TMPA 3B42 v7 (Huffman et al. 2006). Funk et al. (2015) used the inverse distance weighting (IDW) algorithm to blend the satellite and stations data to reduce performance bias. CHIRPS provides daily precipitation at both 0.05° and 0.25° spatial resolution from 1981 to the present. Previous studies suggested that the 0.05° resolution can be used to assess sub-basin and small watersheds (Duan et al. 2016; Aadhar and Mishra 2017; Geleta and Deressa 2021). But at a larger scale, the metrics for both resolutions are similar (Duan et al. 2016). According to the large scale of the case study, the monthly CHIRPS from January 1981 to December 2020 at 0.25° spatial resolution was used. The data were acquired from <ftp://ftp.chg.ucsb.edu>.

Evaluation metrics

The accuracy of the CHIRPS product was evaluated by the coefficient of determination (R²), Pearson Correlation Coefficient (PCC), Root Mean Square Error (RMSE), and Mean Error (ME) as follows:

$$R^2 = \left(\frac{n \sum_{i=1}^n x_{iC} \cdot x_{ig} - \sum_{i=1}^n x_{iC} \sum_{i=1}^n x_{ig}}{\sqrt{n \sum_{i=1}^n x_{iC}^2 - \sum_{i=1}^n x_{iC}^2} \sqrt{n \sum_{i=1}^n x_{ig}^2 - \sum_{i=1}^n x_{ig}^2}} \right)^2 \tag{1}$$

$$PCC = \frac{\sum_{i=1}^n (x_{iC} - \bar{x}_C)(x_{ig} - \bar{x}_g)}{\sqrt{\sum_{i=1}^n (x_{iC} - \bar{x}_C)^2} \sqrt{\sum_{i=1}^n (x_{ig} - \bar{x}_g)^2}} \tag{2}$$

$$RMSE = \sqrt{\frac{\sum_{i=1}^n (x_{iC} - x_{ig})^2}{n}} \tag{3}$$

$$ME = \frac{\sum_{i=1}^n (x_{iC} - x_{ig})}{n} \tag{4}$$

In these equations, x_{iC} and x_{ig} are the CHIRPS and the rain gauges precipitation, respectively. \bar{x}_C and \bar{x}_g are the averages of x_{iC} and x_{ig} and n is the number of observations.

Additionally, the ability of the CHIRPS product to distinguish between rain and no-rain events can be evaluated using Categorical Statistical Indices, including Probability of Detection (POD), False Alarm Ratio (FAR), and Critical Success Index (CSI) (Ebert et al. 2007).

$$POD = \frac{RR}{RR + RN} \tag{5}$$

$$FAR = \frac{NR}{RR + NR} \tag{6}$$

$$CSI = \frac{RR}{RR + RN + NR} \tag{7}$$

In these equations, “R” and “N” indicate rain and no-rain events, respectively. In each combination, the first/second letter represents the station/satellite product. For example, “RN” for a given day shows that the station recorded rainfall, but the product did not detect any rainfall. POD, FAR, and CSI vary between 0 and 1, with the perfect value of 1, 0, and 1, respectively.

Drought characteristic

Drought characteristic is identified by the Run Theory (Yevjevich 1967). Based on this theory, drought can be investigated by Drought Duration (DD), Drought Severity (DS), and Drought Intensity (DI). DD, DS, and DI are identified according to a drought index. In this study, the Standard Precipitation Index (SPI; McKee et al. (1993)) is used. A gamma probability density is firstly fitted to the long-term precipitation series to calculate the SPI:

$$g(x) = \frac{1}{\beta^\alpha \Gamma(\alpha)} x^{\alpha-1} e^{-\frac{x}{\beta}}, \text{ for } x > 0 \tag{8}$$

In this equation, x is the amount of precipitation, and α and β are the shape and scale parameters, respectively. $\Gamma(\alpha)$ is the gamma function presented as follows:

$$\Gamma(\alpha) = \int_0^\infty x^{\alpha-1} e^{-x} dx \tag{9}$$

The best values of α and β are estimated by the maximum likelihood method:

$$\alpha = \frac{1}{4A} \left(1 + \sqrt{1 + \frac{4A}{3}} \right) \tag{10}$$

$$\beta = \frac{\bar{x}}{\alpha} \tag{11}$$

where $A = \ln(\bar{x}) - \frac{\sum \ln(x)}{n}$, \bar{x} and n are the mean and the number of precipitation observations, respectively.

The cumulative probability for a given month can be obtained by the following equation:

$$G(x) = \int_0^x g(x) dx = \frac{1}{\beta^\alpha \Gamma(\alpha)} \int_0^x x^{\alpha-1} e^{-\frac{x}{\beta}} dx \tag{12}$$

And then SPI is calculated as follows:

$$SPI = S \left(t - \frac{c_0 + c_1 t + c_2 t^2}{1 + d_1 t + d_2 t^2 + d_3 t^3} \right) \tag{13}$$

in which, $t = \sqrt{\ln\left(\frac{1}{H(x)}\right)}$, $H(x) = q + (1 - q)G(x)$, and q is the probability of zero rainfall.

For $0 < H(x) \leq 0.5$, $S = -1$, and for $0.5 < H(x) < 1$, $S = 1$. In Eq. 13, $c_0 = 2.5155$, $c_1 = 0.8028$, $c_2 = 0.0103$, $d_1 = 1.4327$, $d_2 = 0.1892$, and $d_3 = 0.0013$.

SPI is calculated by monthly precipitation for different timescales (from 1 to 48 month(s)). In this study, we calculated the SPI for short-term (SPI3, SPI6, and SPI9) and long-term (SPI12, SPI18, and SPI24) droughts. Drought events are characterized by the period with $SPI \leq 0$. The severity of drought events is classified as shown in Table 1.

Table 1 Classification of drought conditions according to the SPI values

SPI value	Drought category
0 to -0.99	Mild drought
-1 to -1.49	Moderate drought
-1.5 to -1.99	Severe drought
≤ -2	Extreme drought

Based on the SPI and Run Theory, DD is defined as the number of months between the start and end of a drought event (when $SPI \leq 0$), DS is the cumulative SPI during DD, and DI is the ratio between DS and DD (i.e., $DI = \frac{DS}{DD}$).

Trend analysis and Sen’s slope estimator

The nonparametric Mann–Kendall test (Mann 1945; Kendall 1975) analyzes the trend in a data time series. The test can be applied to all probability distributions. Thus, the data do not have to meet the assumption of normality. The Mann–Kendall (MK) test is defined as follows:

$$z_{MK} = \begin{cases} \frac{S-1}{\sqrt{V(S)}} & \text{if } S > 0 \\ 0 & \text{if } S = 0 \\ \frac{S+1}{\sqrt{V(S)}} & \text{if } S < 0 \end{cases} \tag{14}$$

where

$$S = \sum_{k=1}^{n-1} \sum_{j=k+1}^n \text{sign}(x_j - x_k) \tag{15}$$

$$V(S) = \frac{[n(n-1)(2n+5) - \sum_{i=1}^m t_i(t_i-1)(2t_i+5)]}{18} \tag{16}$$

In these equations, x_j and x_k are the sequential data values, $V(S)$ is the variance of S , t_i is the number of ties for the i -th value, n and m are the number of data points and tied groups, respectively. The positive/negative value of z_{MK} indicates an upward/downward trend in the series.

The trend magnitude in hydroclimatic data is estimated by the nonparametric Sen’s slope estimator test (Sen 1968) as follows:

$$\beta = \text{Median} \left(\frac{x_j - x_k}{j - k} \right) \tag{17}$$

where x_j and x_k are the time-series value at time j and k ($j > k$). The positive/negative value of β denotes an upward/downward trend (Xu et al. 2010).

Results and discussion

Evaluation of the CHIRPS product

Figures 2 and 3 show that the CHIRPS product provides a reasonable estimation of precipitation at monthly and annual scales; however, it does not perform well on the daily scale. The amount of POD and CSI are less than 0.2 and FAR is higher than 0.6. It shows that CHIRPS could not discriminate between rain and no-rain events. R^2 and PCC at daily scales are less than 0.2 and 0.4, respectively. At monthly and annual scales, R^2 and PCC show higher values (higher than 0.6 and 0.8, respectively), indicating the excellent performance of CHIRPS in monthly and

annual precipitation estimation. The previous studies also found that the satellite products, including CHIRPS, perform better at monthly and annual scales rather than the daily scale (Dembélé and Zwart 2016; Guo et al. 2017; Rivera et al. 2018; Ghozat et al. 2021; Nawaz et al. 2021; Oliveira-Júnior et al. 2021). The precipitation satellite products often use infrared images to detect the temperature of the top of the clouds as part of their algorithm for precipitation estimation. In dry regions, the sensors do not have enough time to detect the temperature of the top of the clouds, because in this regions the clouds disappear very quickly after formation. Hence, the satellite products have a better estimate of precipitation in the wet areas than in the dry areas (Zambrano et al. 2016; Bai et al. 2018). Funk et al. (2015) incorporated the stations' data for bias

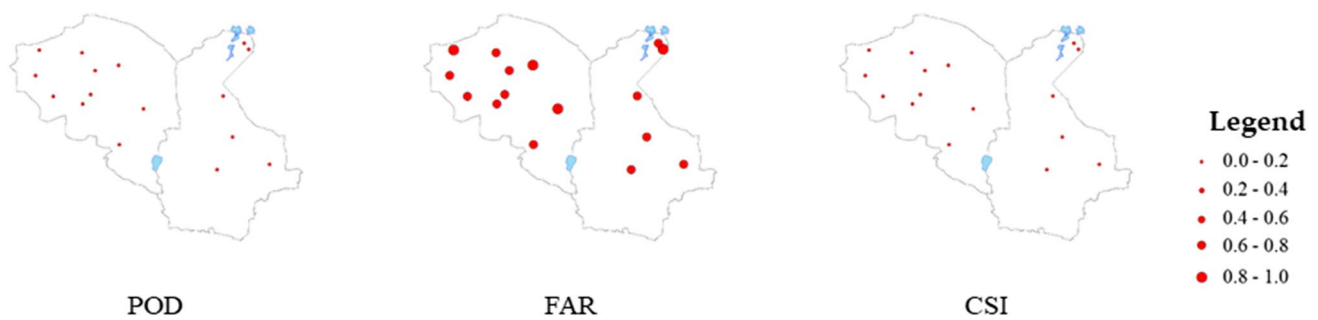


Fig. 2 Categorical Statistical Indices for evaluation of CHIRPS precipitation estimation

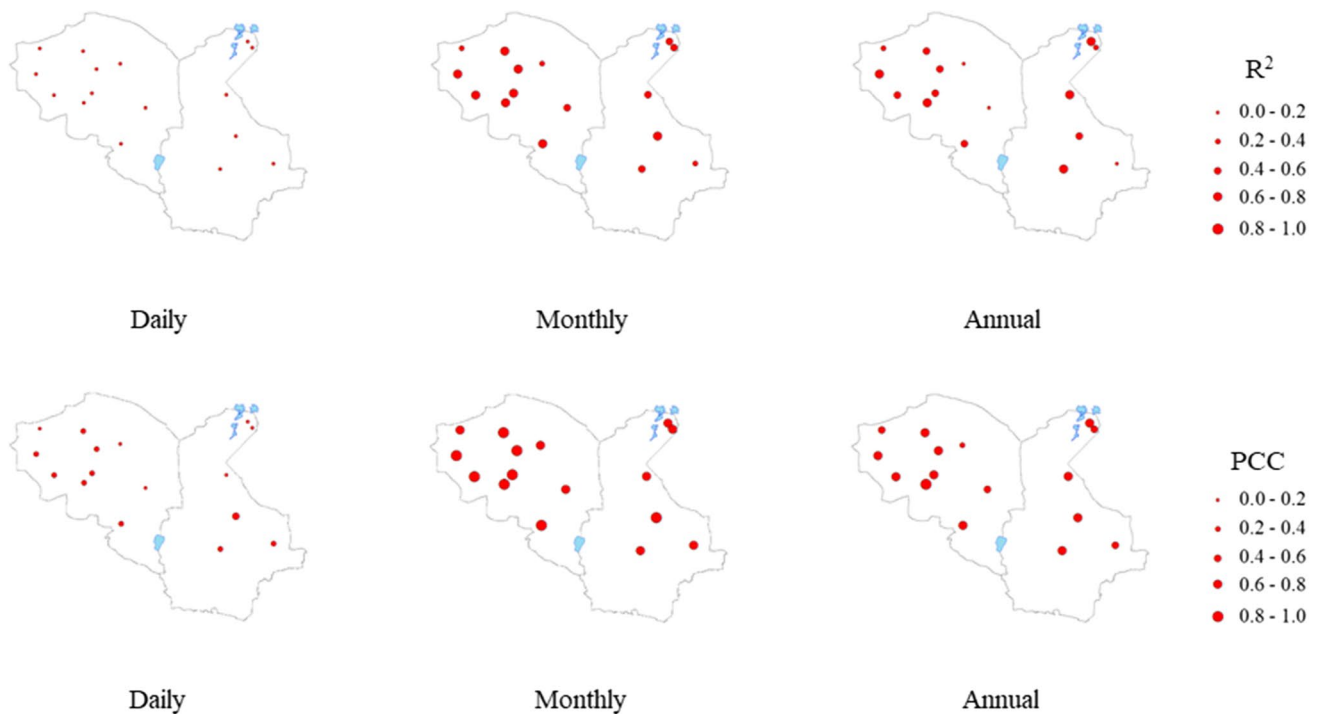


Fig. 3 Comparison of CHIRPS precipitation estimation with rain gauge data using R^2 and PCC

correction by using the IDW algorithm. They believed that the lack of uncertainty information of IDW is a considerable weakness of the CHIRPS algorithm. Thus, they plan to use more rigorous geostatistical models for future CHIRPS releases. They also suggested that the low correlation in parts of Asia, Africa, and South America would be improved by providing more rain gauges (Funk et al. 2015). Moreover, the number of stations used to retrieve precipitation varies significantly from one year to another, and some stations in some countries are located outside the country (Montes et al. 2021). This discrepancy can lead to the inappropriate performance of the CHIRPS product.

Figure 4 shows that RMSE mainly varies between 4–5 mm/day on the daily scale, 10–15 mm/month on the monthly scale, and 40–60 mm/year on the annual scale. The figure also illustrates that ME ranges between -0.2 and +0.2 mm/day on the daily scale, -4 and +4 mm/month on the monthly scale, and -50 and +50 mm/year on the

annual scale. Positive and negative ME values indicate that the model overestimated and underestimated precipitation, respectively. Generally, CHIRPS overestimates precipitation in mountainous stations and underestimates in lowland stations. These results are consistent with previous studies (e.g., Messmer et al. 2021; Nawaz et al. 2021; Geleta and Deressa 2021) and might be because of either local climate or the quality of the rain gauge data (Dinku et al. 2018). However, Saeidizand et al. (2018) showed that compared to the rain gauges rainfall, CHIRPS overestimated precipitation during 2005–2014 in Iran. Figure 5 illustrates the two-dimensional kernel density distribution of the two sets of CHIRPS and rain gauges data. It indicates that for both Kerman (Fig. 5a) and Sistan and Balouchestan (Fig. 5b) Provinces, the CHIRPS-estimated rainfall data captured the rainfall pattern on the monthly scale. Hence, the CHIRPS products work reasonably on the monthly scale and can be applied for drought monitoring over the study region.

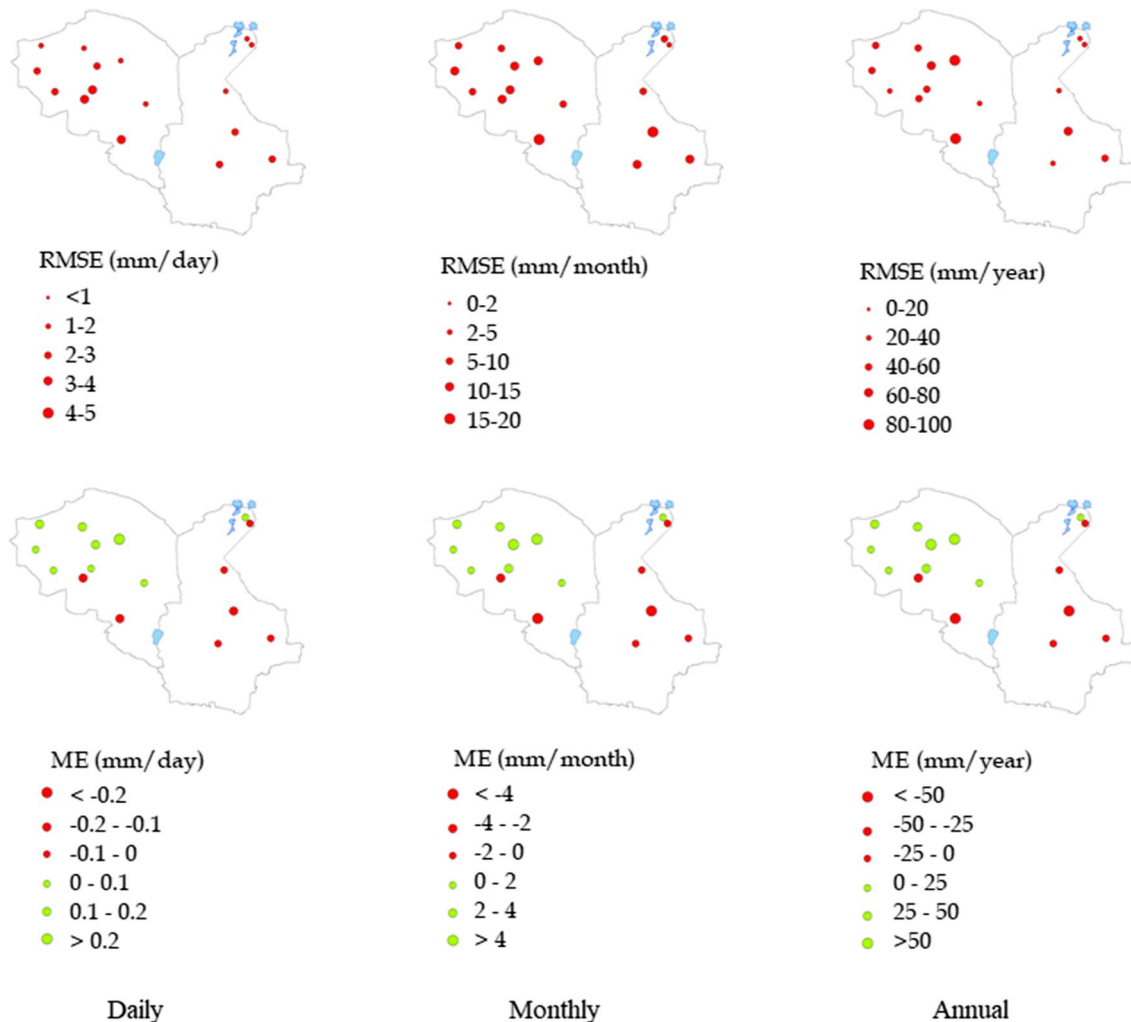


Fig. 4 Comparison of CHIRPS precipitation estimation with rain gauge data by RMSE and ME at daily, monthly, and annual scales

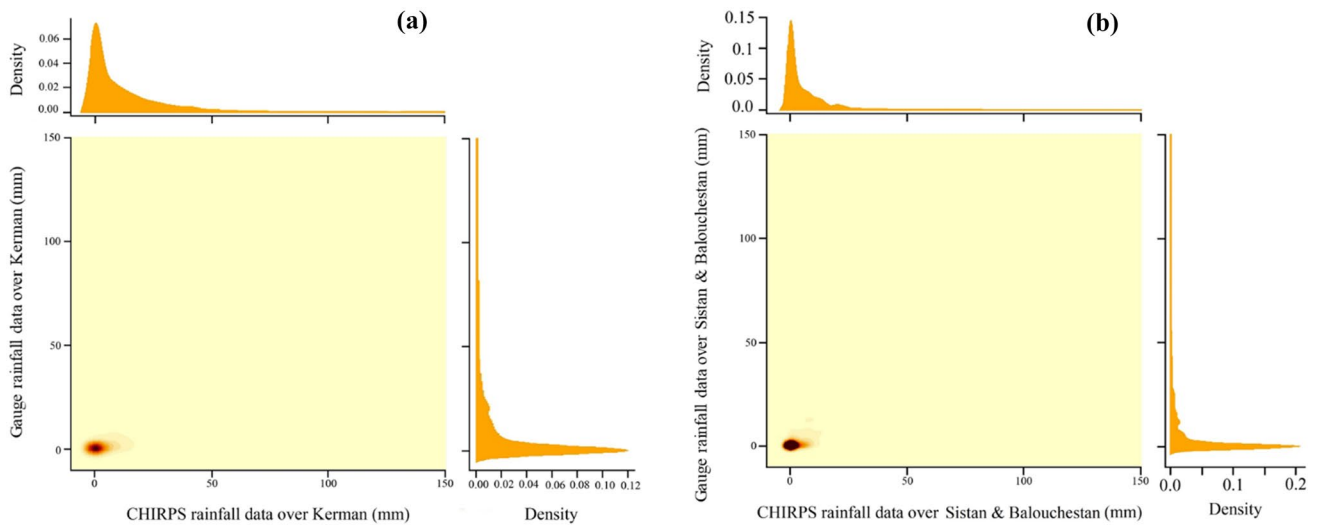


Fig. 5 Two-dimensional kernel density estimate plots for CHIRPS and rain gauge monthly precipitation over **a** Kerman and **b** Sistan and Balouchestan

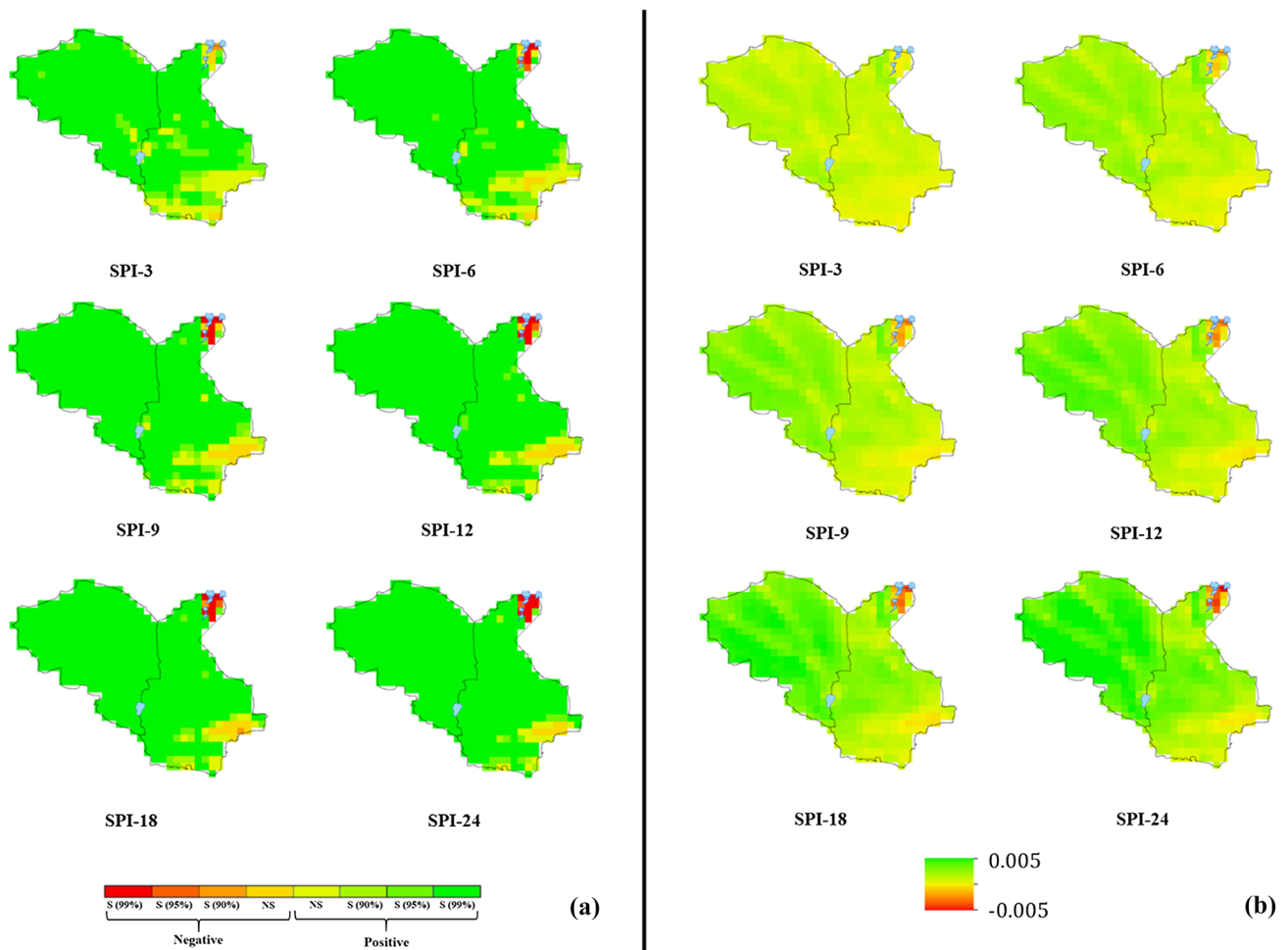
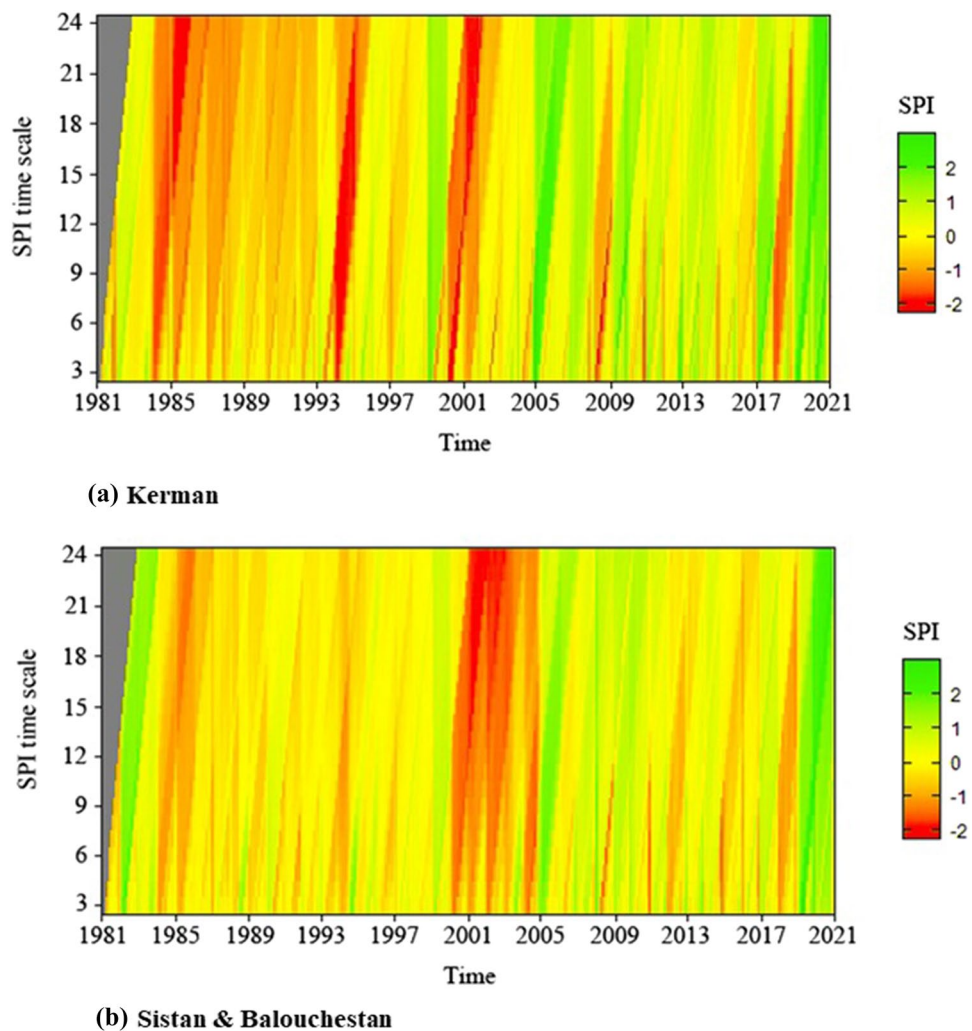


Fig. 6 Spatial distribution of **a** trend and **b** Sen's slope of the SPI time series over the southeast of Iran

Fig. 7 Hovmöller diagram of SPI-1 to SPI-24 for **a** Kerman and **b** Sistan and Balouchestan

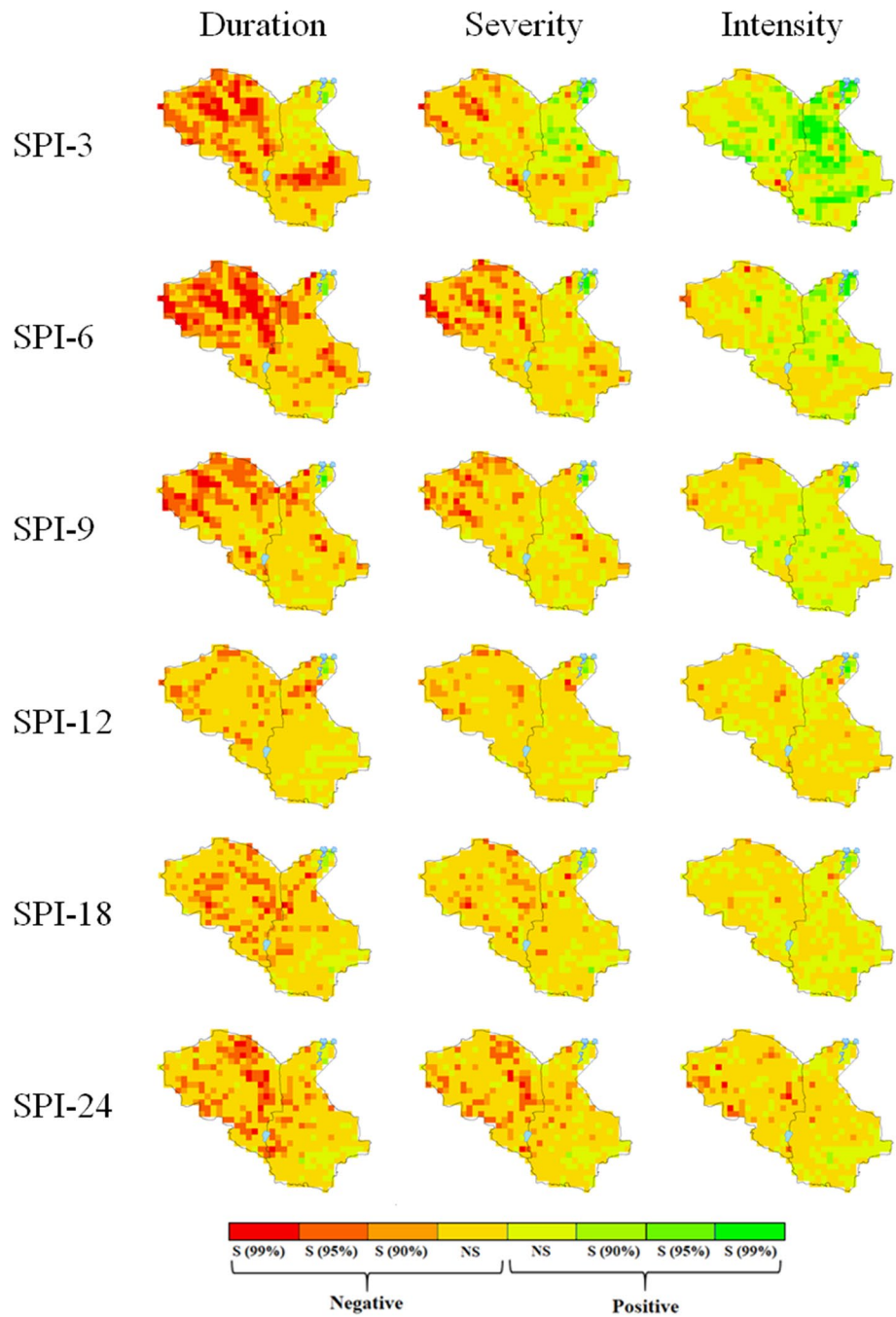


Trends in SPI

Figure 6 shows the spatial distribution of the trend and Sen's slope of the SPI time series over the southeast of Iran. It indicates that SPI has been significantly increasing in this area at all timescales except in some places in the southeast of Sistan and Balouchestan Province, where both increasing and decreasing trends are insignificant (Fig. 6a). However, SPI has been significantly decreasing in the northeast of Sistan and Balouchestan, where Lake Hamoun is located. The results indicate that, generally, the receiving precipitation in southeastern Iran has been increasing during the last four decades. This figure also shows that Sen's slope values and the areas with significant SPI trends increase as the timescale increases (Fig. 6b). It indicates that the long-term droughts show a steeper slope for the SPI time series than the short-term droughts. The spatial distribution of SPI over the four ten-year periods in the southeast of Iran (Fig. S2) confirms this result, as it shows that for all timescales, the fourth decade (2011–2020) is the wettest and the first decade

(1981–1990) is the driest. It is also illustrated by Figs. 7 (Hovmöller diagram) and S3 which provide a visual temporal change in SPI at different timescales during 1981–2020. According to these figures, the shorter timescales exhibit alternating periods of dryness and wetness, since they aggregate periods of lesser drought durations (Qaisrani et al. 2021). In contrast, the longer timescales show more severe and prolonged droughts (Pandey et al. 2021; Qaisrani et al. 2021). The most severe and prolonged drought in both provinces occurred during 1985–1993 and 2000–2004, confirmed by previous studies (Asadi Zarch et al. 2011; Mianabadi et al. 2020). These figures indicate that 2005 to 2020 are the wettest period during the last 40 years. Hence, it may have affected the spatial distribution of Sen's slopes and SPI trends. It may be worth noting that drought events in this area coincide with La Nina, as also confirmed by Nikraftar and Khaniani (2018), Alizadeh-Choobari et al. (2018), Alizadeh-Choobari and Najafi (2018), Amini et al. (2020), and Mohammadrezaei et al. (2020). However, the effect of

Fig. 8 Trends in DD, DS, and DI



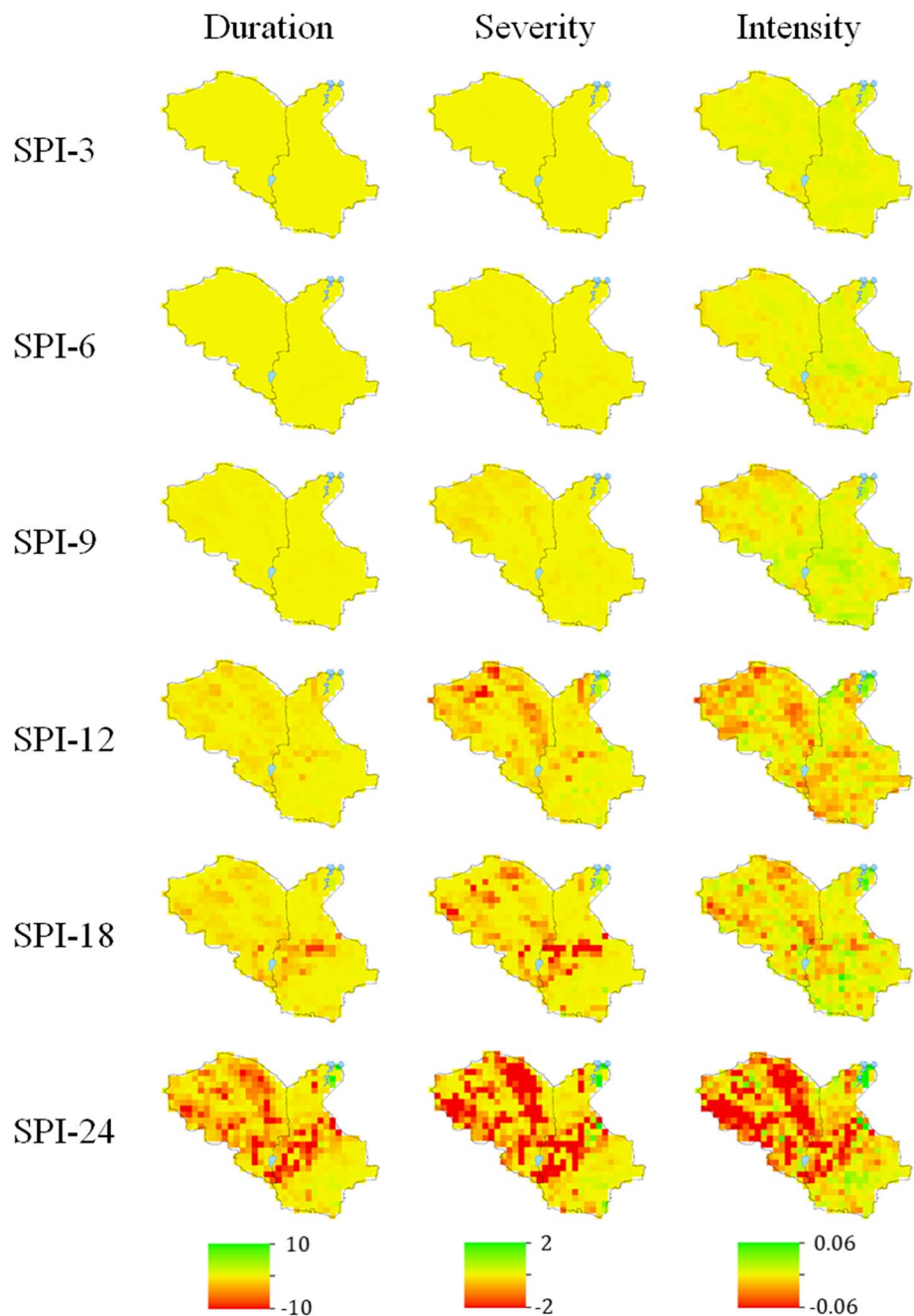
this phenomenon on drought in the southeast of Iran is not remarkable.

Trends in drought characteristics

Figure 8 demonstrates the Z_{MK} value for DD, DS, and DI. It shows that the DD over the southeast of Iran has decreased during these 40 years for short- and long-term droughts. In

the mountainous areas in Kerman, the decreasing trend in DD is significant, especially for SPI-3, SPI-6, and SPI-9. In the north of Sistan and Balouchestan, where Lake Hamoun is located, DD has been increasing, which this increasing trend is mostly insignificant. The results of DS are similar to those of DD; however, the latter have more accentuated trends. Such results were also found by Brasil Neto et al. (2021). They argued that if DD and DS time-series trends are the same, it probably indicates that the trend in DI would

Fig. 9 Sen's slopes for DD, DS, and DI



be constant. This result can be observed in some parts of the study area as well (Fig. 8). Nevertheless, drought events will be more intense when the duration decrease with a greater rate than severity. DS has been increasing for SPI-3 in some regions in Sistan and Balouchestan. This increasing trend is primarily insignificant. At other timescales, DS has an insignificant negative trend. Figure 8 indicates that, in general, DI has been increasing according to SPI-3, SPI-6, and SPI-9 and decreasing according to SPI-12, SPI-18, and SPI-24. It means that the intensity of short-term droughts is increasing, and that of long-term droughts is decreasing. The increasing

trend of DI for SPI-3 is significant, especially over Sistan and Balouchestan. For other scales, both increasing and decreasing trends are insignificant.

In general, the results show that while the duration and severity of short-term droughts (SPI-3, SPI-6, and SPI-9) have been decreasing (i.e., shorter drought events with less severity), their intensity has been increasing. However, changes in duration, severity, and intensity of long-term droughts (SPI-12, SPI-18, and SPI-24) are insignificant. These results are not similar to the results of the SPI trend (Fig. 6a). It is firmly because trend analysis is conducted

with less data in the long-term series than in the short-term series (Brasil Neto et al. 2021). Brasil Neto et al. (2021) argued that a positive trend in SPI does not necessarily lead to a negative trend in the DD time series. Indeed, they complement each other. For example, the results of this study indicate that in some parts of the study area, the long-term events are becoming wetter over time, while their duration tends to be constant.

Figure 9 shows the spatial distribution of Sen's slope for the DD, DS, and DI time series. Regarding the time-scales, the foremost remarkable results of Sen's slopes were observed for long-term droughts. However, trends in DD, DS, and DI are more significant at short-term scales. Such results were found by Brasil Neto et al. (2021) and Qaisrani et al. (2021). Brasil Neto et al. (2021) discussed that reducing the amount of data for these time series may render the series without a high level of significance (e.g., $\alpha > 0.10$), albeit Sen's slopes are rather more accentuated.

Generally, the results of the current study using CHIRPS are similar to the previous studies conducted by Asadi Zarch et al. (2011), Sobhani et al. (2019), and Sharafati et al. (2020), which used rain gauge data for trend analysis of SPI, DD, DS, and DI. Thus, the CHIRPS product can be a reliable alternative data source for drought monitoring in the study area.

Conclusion

The main goal of this study was to detect the drought trends in the southeast of Iran to investigate drought characteristics changes. The nonparametric Mann–Kendall test was used for trend analysis of drought characteristics. Long-term historical precipitation data were collected by applying the CHIRPS satellite precipitation product as independent and alternative sources of ground data. Evaluation of the CHIRPS product showed that it performed better at monthly and annual scales than daily scale. The product also detects the prolonged drought during 1985–1993 and 2000–2004. Thus, it can be applied for drought monitoring, as the monthly precipitation is the primary input for calculating the SPI. The results of drought monitoring during 1981–2020 illustrate that short-term droughts (SPI-3, SPI-6, and SPI-9) have been getting shorter with less severity, while their intensity has increased. However, the increasing trend in DI has been only significant for SPI-3. In contrast, duration, severity, and intensity changes in long-term droughts (SPI-12, SPI-18, and SPI-24) are insignificantly decreasing. In general, it concluded that there had been no significant changes in drought characteristics in the southeast of Iran during the last four decades. The results of this study indicate that the CHIRPS product is a valuable tool for

precipitation estimation and drought monitoring in the study area. Future work can focus on applying other precipitation satellite products to have more reliable results in the study area. It would help the scientists, experts, and decision-makers better distinguish between the role of climate change and human activities on changes in precipitation rate and drought characteristics. It also can lead the policymakers to provide appropriate preparedness plans for dealing with water challenges in the area.

Supplementary Information The online version contains supplementary material available at <https://doi.org/10.1007/s13201-022-01705-4>.

Acknowledgements This research has been supported by the Institute of Science and High Technology and Environmental Sciences, Graduate University of Advanced Technology (Kemran-Iran) under Grant Number of 00/2409.

Funding This research has been supported by the Institute of Science and High Technology and Environmental Sciences, Graduate University of Advanced Technology (Kemran-Iran) under grant number of 00/2409.

Declarations

Conflict of interest The authors have no conflicts of interest to declare.

Consent to participate The authors have read the final manuscript, approved the submission to the journal, and accepted full responsibilities pertaining to the manuscript's delivery and contents.

Ethical approval The manuscript is an original work with its own merit, has not been previously published in whole or in part, and is not being considered for publication elsewhere.

Open Access This article is licensed under a Creative Commons Attribution 4.0 International License, which permits use, sharing, adaptation, distribution and reproduction in any medium or format, as long as you give appropriate credit to the original author(s) and the source, provide a link to the Creative Commons licence, and indicate if changes were made. The images or other third party material in this article are included in the article's Creative Commons licence, unless indicated otherwise in a credit line to the material. If material is not included in the article's Creative Commons licence and your intended use is not permitted by statutory regulation or exceeds the permitted use, you will need to obtain permission directly from the copyright holder. To view a copy of this licence, visit <http://creativecommons.org/licenses/by/4.0/>.

References

- Aadhar S, Mishra V (2017) High-resolution near real-time drought monitoring in South Asia. *Sci Data* 4:170145. <https://doi.org/10.1038/sdata.2017.145>
- Afzal M, Ragab R (2020) Assessment of the potential impacts of climate change on the hydrology at catchment scale: modelling approach including prediction of future drought events using drought indices. *Appl Water Sci* 10:215. <https://doi.org/10.1007/s13201-020-01293-1>
- Ahmad HQ, Kamaruddin SA, Harun SB et al (2021) Assessment of spatiotemporal variability of meteorological droughts in

- Northern Iraq using satellite rainfall data. *KSCE J Civ Eng*. <https://doi.org/10.1007/s12205-021-2046-x>
- Alizadeh-Choobari O, Najafi MS (2018) Climate variability in Iran in response to the diversity of the El Niño-Southern Oscillation. *Int J Climatol* 38:4239–4250. <https://doi.org/10.1002/joc.5564>
- Alizadeh-Choobari O, Zavar-Reza P, Sturman A (2014) The “wind of 120days” and dust storm activity over the Sistan Basin. *Atmos Res* 143:328–341. <https://doi.org/10.1016/j.atmosres.2014.02.001>
- Alizadeh-Choobari O, Adibi P, Irannejad P (2018) Impact of the El Niño-Southern Oscillation on the climate of Iran using ERA-Interim data. *Clim Dyn* 51:2897–2911. <https://doi.org/10.1007/s00382-017-4055-5>
- Amini M, Ghadami M, Fathian F, Modarres R (2020) Teleconnections between oceanic-atmospheric indices and drought over Iran using quantile regressions. *Hydrol Sci J* 65:2286–2295. <https://doi.org/10.1080/02626667.2020.1802029>
- Asadi Zarch MA, Malekinezhad H, Mobin MH et al (2011) Drought monitoring by reconnaissance drought index (RDI) in Iran. *Water Resour Manag* 25:3485–3504. <https://doi.org/10.1007/s11269-011-9867-1>
- Ayehu GT, Tadesse T, Gessesse B, Dinku T (2018) Validation of new satellite rainfall products over the Upper Blue Nile Basin, Ethiopia. *Atmos Meas Tech* 11:1921–1936. <https://doi.org/10.5194/amt-11-1921-2018>
- Bai L, Shi C, Li L et al (2018) Accuracy of CHIRPS satellite-rainfall products over Mainland China. *Remote Sens* 10:362. <https://doi.org/10.3390/rs10030362>
- Balist J, Malekmohammadi B, Jafari HR et al (2022) Detecting land use and climate impacts on water yield ecosystem service in arid and semi-arid areas. A study in Sirvan River Basin-Iran. *Appl Water Sci* 12:1–14. <https://doi.org/10.1007/s13201-021-01545-8>
- Brasil Neto RM, Santos CAG, da Silva JFCB, C, et al (2021) Evaluation of the TRMM product for monitoring drought over Paraíba State, northeastern Brazil: a trend analysis. *Sci Rep* 11:1–18. <https://doi.org/10.1038/s41598-020-80026-5>
- Burroughs W (2003) *Climate: into the 21st century*. Cambridge University Press, Cambridge, UK
- Delju AH, Ceylan A, Piguat E, Rebetez M (2013) Observed climate variability and change in Urmia Lake Basin. *Iran Theor Appl Climatol* 111:285–296. <https://doi.org/10.1007/s00704-012-0651-9>
- Dembélé M, Zwart SJ (2016) Evaluation and comparison of satellite-based rainfall products in Burkina Faso, West Africa. *Int J Remote Sens* 37:3995–4014. <https://doi.org/10.1080/01431161.2016.1207258>
- Derdous O, Bouamrane A, Mrad D (2021) Spatiotemporal analysis of meteorological drought in a Mediterranean dry land: case of the Cheliff basin–Algeria. *Model Earth Syst Environ* 7:135–143. <https://doi.org/10.1007/s40808-020-00951-2>
- Dinku T, Funk C, Peterson P et al (2018) Validation of the CHIRPS satellite rainfall estimates over eastern Africa. *Q J R Meteorol Soc* 144:292–312. <https://doi.org/10.1002/qj.3244>
- Duan Z, Liu J, Tuo Y et al (2016) Evaluation of eight high spatial resolution gridded precipitation products in Adige Basin (Italy) at multiple temporal and spatial scales. *Sci Total Environ* 573:1536–1553. <https://doi.org/10.1016/j.scitotenv.2016.08.213>
- Ebert EE, Janowiak JE, Kidd C (2007) Numerical models. *Bull Am Meteorol Soc* 88:47–64. <https://doi.org/10.1175/BAMS-88-I-47>
- Eslami Z, Janatrostami S, Ashrafzadeh A, Poumohamad Y (2020) Water, energy, food nexus approach impact on integrated water resources management in sefid-rud irrigation and drainage network. *J Water Soil* 34:11–25. <https://doi.org/10.22067/jsw.v34i1.81897>
- Funk C, Peterson P, Landsfeld M et al (2015) The climate hazards infrared precipitation with stations - A new environmental record for monitoring extremes. *Sci Data* 2:1–21. <https://doi.org/10.1038/sdata.2015.66>
- Gao F, Zhang Y, Ren X et al (2018) Evaluation of CHIRPS and its application for drought monitoring over the Haihe River Basin, China. *Nat Hazards* 92:155–172. <https://doi.org/10.1007/s11069-018-3196-0>
- Geleta CD, Deressa TA (2021) Evaluation of climate hazards group infrared precipitation station (CHIRPS) <scp>satellite-based</scp> rainfall estimates over Fincha and Neshe Watersheds, Ethiopia. *Eng Reports* 3:1–16. <https://doi.org/10.1002/eng2.12338>
- Ghandehari A, Davary K, Khorasani HO et al (2020) Assessment of urban water supply options by using fuzzy possibilistic theory. *Environ Process*. <https://doi.org/10.1007/s40710-020-00441-8>
- Ghozat A, Sharafati A, Hosseini SA (2021) Long-term spatiotemporal evaluation of CHIRPS satellite precipitation product over different climatic regions of Iran. *Theor Appl Climatol* 143:211–225. <https://doi.org/10.1007/s00704-020-03428-5>
- Greve P, Orłowsky B, Mueller B et al (2014) Global assessment of trends in wetting and drying over land. *Nat Geosci* 7:716–721. <https://doi.org/10.1038/ngeo2247>
- Guo H, Bao A, Liu T et al (2017) meteorological drought analysis in the lower mekong basin using satellite-based long-term CHIRPS product. *Sustainability* 9:901. <https://doi.org/10.3390/su9060901>
- Heathcote R (1983) *The arid lands: their use and abuse*. Longman, New York
- Huffman GJ, Adler RF, Bolvin DT et al (2006) The TRMM multisatellite precipitation analysis (TMPA): quasi-global, multiyear, combined-sensor precipitation estimates at fine scales. *J Hydro-meteorol* 8:38–55. <https://doi.org/10.1175/JHM560.1>
- Kassaye AY, Shao G, Wang X, Wu S (2021) Quantification of drought severity change in Ethiopia during 1952–2017. *Environ Dev Sustain* 23:5096–5121. <https://doi.org/10.1007/s10668-020-00805-y>
- Kendall MG (1975) *Rank correlation methods*. Charles Griffin, London, UK
- Kolahi M, Sakai T, Moriya K, Makhdoum MF (2012) Challenges to the future development of Iran’s protected areas system. *Environ Manage* 50:750–765
- Liu C, Yang C, Yang Q, Wang J (2021) Spatiotemporal drought analysis by the standardized precipitation index (SPI) and standardized precipitation evapotranspiration index (SPEI) in Sichuan Province, China. *Sci Rep* 11:1–14. <https://doi.org/10.1038/s41598-020-80527-3>
- Lotfirad M, Adib A, Salehpoor J et al (2021) Simulation of the impact of climate change on runoff and drought in an arid and semiarid basin (the Hablehroud, Iran). *Appl Water Sci* 11:1–24. <https://doi.org/10.1007/s13201-021-01494-2>
- Madani K (2014) Water management in Iran: what is causing the looming crisis? *J Environ Stud Sci* 4:315–328. <https://doi.org/10.1007/s13412-014-0182-z>
- Madani K, Aghakouchak A, Mirchi A (2016) Iran’s Socio-economic drought: challenges of a Water-Bankrupt Nation. *Iran Stud* 49:997–1016
- Mahajan DR, Dodamani BM (2015) Trend analysis of drought events over upper Krishna Basin in Maharashtra. *Aquat Procedia* 4:1250–1257. <https://doi.org/10.1016/j.aqpro.2015.02.163>
- Makhdoum MF (2008) Management of protected areas and conservation of biodiversity in Iran. *Int J Environ Stud* 65:563–585. <https://doi.org/10.1080/00207230802245898>
- Mann HB (1945) Nonparametric tests against trend. *Econometrica* 13:245–259
- McKee TB, Doesken NJ, Kleist J (1993) The relationship of drought frequency and duration of time scales. In: Eighth conference on applied climatology, American Meteorological Society Jan 17–23:179–186
- Messmer M, González-Rojí SJ, Raible CC, Stocker TF (2021) Sensitivity of precipitation and temperature over the Mount Kenya area to physics parameterization options in a high-resolution model simulation performed with WRFV3.8.1. *Geosci Model Dev* 14:2691–2711. <https://doi.org/10.5194/gmd-14-2691-2021>

- Mianabadi H, Mostert E, Van De Giesen N (2015) Trans-boundary river basin management : factors influencing the success or failure of international agreements. In: Hipel WK, Fang L, Cullmann J, Bristow M (eds) Conflict resolution in water resources and environmental management. Springer, Heidelberg, pp 133–143
- Mianabadi A, Shirazi P, Ghahraman B et al (2019) Assessment of short- and long-term memory in trends of major climatic variables over Iran: 1966–2015. *Theor Appl Climatol* 135:677–691. <https://doi.org/10.1007/s00704-018-2410-z>
- Mianabadi A, Davary K, Mianabadi H, Karimi P (2020) International Environmental Conflict Management in Transboundary River Basins. *Water Resour Manag* 34:3445–3464. <https://doi.org/10.1007/s11269-020-02576-7>
- Mianabadi A, Davary K, Kolahi M, Fisher J (2021) Water/climate nexus environmental rural-urban migration and coping strategies. *J Environ Plan Manag*. <https://doi.org/10.1080/09640568.2021.1915259>
- Mianabadi A, Salari K, Pourmohamad Y (2022) Evaluation of CHIRPS satellite product for trend analysis of precipitation in the Southeast of Iran. *Iran J Irrig Drain* accepted f:
- Mohammadrezaei M, Soltani S, Modarres R (2020) Evaluating the effect of ocean-atmospheric indices on drought in Iran. *Theor Appl Climatol* 140:219–230. <https://doi.org/10.1007/s00704-019-03058-6>
- Montes C, Acharya N, Hassan SMQ, Krupnik TJ (2021) Intense precipitation events during the monsoon season in Bangladesh as captured by satellite-based products. *J Hydrometeorol* 22:1405–1419. <https://doi.org/10.1175/JHM-D-20-0287.1>
- Najjuma M, Nimusiima A, Sabiiti G, Opio R (2021) Characterization of historical and future drought in central uganda using CHIRPS rainfall and RACMO22T model data. *Int J Agric* for 11:9–15. <https://doi.org/10.5923/j.ijaf.20211101.02>
- Nawaz M, Iqbal MF, Mahmood I (2021) Validation of CHIRPS satellite-based precipitation dataset over Pakistan. *Atmos Res* 248:105289. <https://doi.org/10.1016/j.atmosres.2020.105289>
- Nikraftar Z, Khaniani AS (2018) Assessing the impact of cold and warm ENSO on drought over Iran. *Earth Obs Geomatics Eng* 2:45–55. <https://doi.org/10.22059/eoge.2018.257714.1022>
- Oliveira-Júnior JF, Silva Junior CA, Teodoro PE et al (2021) Confronting CHIRPS dataset and in situ stations in the detection of wet and drought conditions in the Brazilian Midwest. *Int J Climatol*. <https://doi.org/10.1002/joc.7080>
- Oliver-Smith A (2012) Debating environmental migration: society, nature and population displacement in climate change. *J Int Dev* 24:1058–1070. <https://doi.org/10.1002/jid.2887>
- Pandey V, Srivastava PK, Singh SK et al (2021) Drought identification and trend analysis using long-term chirps satellite precipitation product in bundelkhand, india. *Sustain* 13:1–20. <https://doi.org/10.3390/su13031042>
- Pathak AA, Dodamani BM (2020) Trend analysis of rainfall, rainy days and drought: a case study of Ghataprabha River Basin, India. *Model Earth Syst Environ* 6:1357–1372. <https://doi.org/10.1007/s40808-020-00798-7>
- Pourmohamad Y, Shahnazari A, Emadi AR, Ahmadi MZ (2012) Effect of dredging of Wetlands on variation of water allocation in Alborz Dam watershed using WEAP model. *J Watershed Manag Res* 2:44–56
- Pourmohamad Y, Alizadeh A, Mousavi Baygi M et al (2019) Optimizing cropping area by proposing a combined water-energy productivity function for Neyshabur Basin. *Iran Agric Water Manag* 217:131–140. <https://doi.org/10.1016/j.agwat.2019.02.040>
- Pourmohamad Y, Ghandehari A, Davary K, Shirazi P (2020) Multicriteria decision-making approach to enhance automated anchor pixel selection algorithm for arid and semi-arid regions. *J Hydrol Eng* 25:04020049. [https://doi.org/10.1061/\(asce\)he.1943-5584.0002006](https://doi.org/10.1061/(asce)he.1943-5584.0002006)
- Qaisrani ZN, Nuthammachot N, Techato K, Asadullah, (2021) Drought monitoring based on standardized precipitation index and standardized precipitation evapotranspiration Index in the arid zone of Balochistan province. *Pakistan Arab J Geosci*. <https://doi.org/10.1007/s12517-020-06302-w>
- Rashki A (2012) Seasonality and mineral, chemical and optical properties of dust storms in the Sistan region of Iran, and their influence on human health. University of Pretoria
- Rivera JA, Marianetti G, Hinrichs S (2018) Validation of CHIRPS precipitation dataset along the Central Andes of Argentina. *Atmos Res* 213:437–449. <https://doi.org/10.1016/j.atmosres.2018.06.023>
- Saeidizand R, Sabetghadam S, Tarnavsky E, Pierleoni A (2018) Evaluation of CHIRPS rainfall estimates over Iran. *Q J R Meteorol Soc* 144:282–291. <https://doi.org/10.1002/qj.3342>
- Safaei V, Pourmohammad Y, Davary K (2020) Integrated approach of water, energy and food in water resources management (Case Study: Mashhad Catchment). *Iran J Irrig Drain* 14:1708–1721
- Sandeep P, Obi Reddy GP, Jegankumar R, Arun Kumar KC (2021) Monitoring of agricultural drought in semi-arid ecosystem of Peninsular India through indices derived from time-series CHIRPS and MODIS datasets. *Ecol Indic* 121:107033. <https://doi.org/10.1016/j.ecolind.2020.107033>
- Santos CAG, Brasil Neto RM, Nascimento TVM, do, et al (2021) Geospatial drought severity analysis based on PERSIANN-CDR-estimated rainfall data for Odisha state in India (1983–2018). *Sci Total Environ* 750:141258. <https://doi.org/10.1016/j.scitotenv.2020.141258>
- Sen PK (1968) Estimates of the regression coefficient based on Kendall's Tau. *J Am Stat Assoc* 63:13799–21389. <https://doi.org/10.2307/2285891>
- Sharafati A, Nabaei S, Shahid S (2020) Spatial assessment of meteorological drought features over different climate regions in Iran. *Int J Climatol* 40:1864–1884. <https://doi.org/10.1002/joc.6307>
- Sharma A, Goyal MK (2020) Assessment of drought trend and variability in India using wavelet transform. *Hydrol Sci J* 65:1539–1554. <https://doi.org/10.1080/02626667.2020.1754422>
- Sobhani B, Zengir VS, Kianian MK (2019) Iranian (Iranica) journal of energy & environment modeling, monitoring and prediction of drought in Iran. *Iran J Energy Environ* 10:216–224
- UNFCCC (2007) Climate change: impacts, vulnerabilities and adaptation in developing countries. United Nations Framework Conv Clim Chang
- WMO (2013) The global climate 2001 – 2010
- Xu C, Widén E, Halldin S (2005) Modelling hydrological consequences of climate change—Progress and challenges. *Adv Atmos Sci* 22:789–797. <https://doi.org/10.1007/BF02918679>
- Xu K, Milliman JD, Xu H (2010) Temporal trend of precipitation and runoff in major Chinese Rivers since 1951. *Glob Planet Change* 73:219–232. <https://doi.org/10.1016/j.gloplacha.2010.07.002>
- Yevjevich V (1967) An objective approach to definitions and investigations of continental hydrologic droughts. *Hydrol Pap* 23:1–18
- Zambrano F, Wardlow B, Tadesse T (2016) Evaluating satellite-derived long-term historical precipitation datasets for drought monitoring in Chile. In: Neale CMU, Maltese A (eds) Remote Sensing for Agriculture, Ecosystems, and Hydrology XVIII, 9998. p 999823
- Zerouali B, Chettih M, Abda Z et al (2021) Spatiotemporal meteorological drought assessment in a humid Mediterranean region: case study of the Oued Sebaou basin (northern central Algeria). *Nat Hazards* 108:689–709. <https://doi.org/10.1007/s11069-021-04701-0>
- Zhao Y, Norouzi H, Azarderakhsh M, AghaKouchak A (2021) Global patterns of hottest, coldest, and extreme diurnal variability on earth. *Bull Am Meteorol Soc* 102:E1672–E1681. <https://doi.org/10.1175/bams-d-20-0325.1>